Fire Technology, 46, 251–274, 2010

DOI: 10.1007/s10694-009-0088-6

Fire Induced Spalling in High Strength Concrete Beams

M. B. Dwaikat and V. K. R. Kodur, Department of CEE, Michigan State University, East Lansing, MI, USA,*
e-mail: kodur@egr.msu.edu

Received: 17 October 2008/**Accepted:** 1 March 2009

Abstract. A macroscopic finite element model is extended to account for fire induced spalling in high strength concrete (HSC) beams. The model is based on the principles of mechanics and thermodynamics and utilizes pore pressure calculations to predict fire induced spalling in concrete. For validating the model, spalling measurements were made by conducting fire resistance experiments on four normal strength and high strength concrete beams. Spalling predictions from the model are compared with the measured values of spalling at various stages of fire exposure. The validated model is applied to investigate the influence of fire scenario, concrete strength (permeability) and axial restraint on the fire induced spalling and fire response of RC beams. Results from the analysis show that fire scenario, and concrete permeability largely influence the extent of fire induced spalling in concrete beams. Further, it is also shown that the extent of spalling has significant influence on the fire resistance of RC beams.

Keywords: fire induced spalling, high strength concrete, pore pressure, numerical model, fire resistance, concrete beams

1. Introduction

Reinforced concrete structural systems are quite frequently used in high rise buildings and other built infrastructure due to the advantages concrete construction offers over other materials. When used in buildings, provision of appropriate fire safety measures for structural members is an important aspect of design since fire represents one of the most severe environmental conditions to which structures may be subjected. The basis for this requirement can be attributed to the fact that, when other measures for containing the fire fail, structural integrity is the last line of defense.

In recent years, high strength concrete (HSC) is being widely used in place of normal strength concrete (NSC), due to significant economic, architectural, and structural advantages HSC can provide as compared to conventional NSC. With the increased use of HSC, concern has developed regarding the behavior of such concretes under fire exposure. The occurrence of fire induced spalling is one of the major reasons for this concern.

* Correspondence should be addressed to: M. B. Dwaikat, E-mail: dwaikatm@msu.edu

Generally, concrete structural members (mainly comprising of NSC) exhibit good performance under fire situations. However, HSC may not exhibit the same level of performance (as that of NSC) under severe fire conditions [1, 2]. This is mainly due to faster degradation of strength properties at high temperatures and also due to the occurrence of fire induced spalling. While spalling can occur in all concrete types when exposed to rapid heating (such as the one encountered in fires), results from a number of studies [3–8] have shown that HSC is more susceptible to fire induced spalling than NSC. The high compactness and low permeability of HSC (often due to the presence of silica fume) accelerate the pore pressure development leading to spalling, that can be explosive under some conditions. Such spalling has the effect of reducing the cross sectional area of the structural member, and increasing the heat penetration to the steel reinforcement. Thus, spalling might lead to reduction in strength and stiffness of RC structural members, which in turn might cause early failure of RC members under fire conditions [1].

Fire induced spalling in concrete structures have been observed both in laboratory experiments and under real fire conditions [5, 9]. At present, there is very limited guidance on the approaches to incorporate spalling in fire resistance calculations [10]. This is mainly due to lack of calculations methodologies and reliable high temperature material properties for modeling spalling progression in concrete.

In this paper, a macroscopic finite element model, developed originally for evaluating the fire response of RC members, is extended to account for fire induced spalling in RC beams. The spalling submodel, incorporate into the macroscopic finite element model, is based on principles of mechanics and thermodynamics and compute pore pressure by taking into consideration varying permeability distribution across the cross section of an RC beam. The model is validated against data from fire resistance experiments on four RC beams. The validated model is applied to investigate the effect of critical parameters, namely; concrete permeability and strength, fire scenario and axial restraint on fire induced spalling and on overall fire resistance of RC beams.

2. Fire Induced Spalling in Concrete

Reinforced concrete members, when exposed to fire, experience increasing temperatures with time. The increasing temperatures lead to gradual loss of strength and stiffness properties in concrete and ultimately lead to failure. However, under some conditions, chunks of concrete might break-up from the structural member during exposure to fire. This break-up of concrete is termed as fire induced spalling and primarily results from the build-up of pore pressure within the concrete. The occurrence of such spalling is dependent on a number of factors including fire conditions.

The occurrence of spalling in concrete members can broadly be classified into three stages, namely; early spalling, intermediate spalling, and late spalling. Early spalling can start after 5–10 min of fire exposure and can continue up to

30–45 min. This type of spalling is generally of explosive nature and often results due to the development of high thermal gradients within the parts of concrete members. Early spalling results in the break-up of large chunks of concrete and thus may have detrimental effect on the fire resistance of RC members particularly when spalling reduces the concrete cover thickness to the main reinforcement. Intermediate spalling that occurs after about 30–45 min of fire exposure results in the form of surface scaling (breaking off small pieces of concrete) and this can continue through final stages of fire exposure. Such type of spalling has less effect on the fire resistance of RC members because this type of spalling generally results in break-up of thin layers of concrete. Late spalling occurs just prior to failure of structural members and primarily results from significant loss of strength and stiffness of concrete and reinforcement due to exposure to fire. Hence, this spalling has minor influence on the overall fire response of RC members.

A review of literature presents a conflicting picture on the frequency of occurrence of spalling and also on the exact mechanism for spalling [1]. While many research studies illustrated explosive spalling in concrete members under laboratory conditions, there are a few other studies which report little or no significant spalling. One possible explanation for this confusing trend of observations is the large number of factors that influence spalling and also the inter-dependency of some of these factors. However, most researchers agree that the primary reasons for occurrence of spalling are low permeability of concrete and moisture migration at elevated temperatures [1–3].

Permeability of concrete depends on many factors including porosity, pore size distribution, connectivity of the pores, and tortuosity of the concrete pores. Thus, concretes with similar level of porosity, can have different degrees of permeability due to variations in other factors. Typically, NSC with a compressive strength in the range of 20–70 MPa, can have permeability in the range of 10^{-13} to 10^{-16} m^2, while HSC with strength above 70 MPa can have permeability in the range of 10^{-16} to 10^{-20} m^2 [11]. Permeability also depends on the extent of cracking (including distribution) and damage in concrete members. For RC beams at room temperature, the cracking and damage may not be uniform within the cross section of the beam due to the non-uniform stress distribution caused by varying bending moment. This leads to a significant variation in the concrete permeability within the cross section of the beam.

In addition, the common practice for curing RC beams is by using burlap soaked with water on the top surface of the beam. Despite the fact that the bond strength, and thus the tensile strength of concrete, may be less for the top part of the beam mainly due to segregation of concrete while casting, using burlap for curing significantly reduces the evaporation of water from the top part of concrete and provides better curing conditions. This may influence the permeability variation within the beam cross section. The variation in permeability largely influences the extent of fire induced spalling in the beam cross section and hence the overall fire response of the beam. Another factor that influences the fire induced spalling is the fire intensity and rate of temperature rise. The rate of heating significantly influences the thermal gradient and thus the build-up of pore pressure in the concrete section which largely affects the extent of spalling.

In the last two decades, there have been several experimental studies to investigate fire induced spalling in HSC. Some of these studies were conducted on small scale specimens such as those conducted by Phan [12], Han et al. [13], Hertz [14], and Phan et al. [15]. Other studies were conducted on building components (columns and concrete blocks) such as those reported by Park et al. [16], Kodur [17], Kodur and McGrath [18], and Kodur et al. [19], Bilodeau et al. [20]. All these studies have shown that HSC members are generally more susceptible to spalling as compared to NSC members. These studies focused mostly on RC columns under standard fire scenarios, without any consideration for cooling phase of the fire exposure. Further, there have been no experimental studies to investigate fire induced spalling in HSC beams under design fire scenarios.

The literature review also indicates that there have been limited analytical models to predict spalling in concrete members [21]. Some researchers have developed complex spalling models that are based on hydro-thermo-mechanical analysis and involve undertaking pore pressure calculations [22–26]. For such models to accurately predict the pore pressure inside concrete, material properties such as concrete permeability tensor, diffusion coefficients, material stiffness tensor, must be precisely known. These properties vary as a function of temperature. But, many of these properties are not well defined even at room temperature [21]. Thus, it is almost impossible to predict spalling using the available model due to the lack of high temperature properties.

In lieu of complex hydro-thermo-mechanical models, some researchers proposed simplified thumb rules [27] based on temperature calculations in concrete without any consideration to pore pressure development. These thumb rules were developed based on spalling observations in fire tests (on RC columns) and correlating them with temperature rise in the cross section. Due to significant inaccuracies associated with monitoring spalling during fire tests, these models may not provide reasonable prediction of spalling. Also, these spalling thumb rules were primarily developed based on either small scale specimens or RC columns, and may not applicable for RC beams. Thus, the currently available spalling models (hydro-thermo-mechanical models and simplified approaches) are of limited practical use [21].

There is very limited guidance in current codes and standards for predicting fire induced spalling in concrete. Some codes and standards include broad guidelines for estimating and mitigating spalling. As an illustration, Eurocode specifications [28] state that spalling is unlikely to occur when the moisture content of concrete is lower than 3%, without any due consideration to permeability and the tensile strength of concrete. Similarly, ACI 216.1 standard [29] does not have any specifications for predicting when spalling might occur. However, this standard provides some guidelines for mitigating spalling in HSC through the use of polypropylene fibers in concrete mix. It should be noted that the guidelines on spalling in current codes are mainly derived based on observations during fire tests on small specimens and do not give consideration to critical factors that influence this phenomenon. One of the main reasons for slow progress in developing rational methods for predicting spalling, and also for developing solutions to mitigate spalling, is the lack of calculation methodologies for predicting spalling.

3. Numerical Model

3.1. General

A macroscopic finite element model, originally developed for modeling the fire response of RC beams, is extended to account for fire induced spalling in RC beams. In the model, the RC beam is divided into a number of segments along its length and the mid-section of the segment is assumed to represent the behavior of the whole segment. The cross section, representing each segment, is subdivided into elements forming a two dimensional mesh. The fire resistance analysis is carried out by incrementing time in steps. At each time interval, the analysis is performed through three main steps:

– Establishing fire temperature due to fire exposure,
– Carrying out coupled heat transfer-spalling analysis in each segment to predict cross sectional temperature and spalling, and
– Performing strength and deflection analysis, which is carried out, through three substeps:

  - Calculating the axial restraint force in the RC beam,
  - Generation of moment-curvature relationships (utilizing the axial restraint force computed above) for each beam segment, and
  - Performing structural analysis of the beam to compute deflections and internal forces.

A spalling submodel was incorporated in the model to account for fire induced spalling in concrete. In the spalling submodel, hydrothermal analysis is carried out to compute the pore pressure in the beam cross section [21]. When the pore pressure exceeds the temperature dependent tensile strength of concrete, tensile fracture occurs in the concrete which leads to breaking off of concrete layers (segments) from the RC beam. In the previous version of the spalling submodel, the permeability of concrete was assumed to be uniform over the concrete cross section at room temperature. In this paper, the spalling submodel is extended to account for the variation of permeability in the section of the beam which results from cracking and curing conditions. More details on the model extension are given the following section. Full details of the numerical procedure, including the derivation of appropriate equations, are presented elsewhere [21, 30].

3.2. Spalling Submodel

The proposed spalling submodel is based on hydrothermal analysis and computes pore pressure within the cross section at any given fire exposure time. The analysis utilizes the principles of mechanics and thermodynamics, including the conservation of mass of liquid water and water vapor, to compute pore pressure in the concrete resulting from fire exposure. In the hydrothermal model, the mass transfer equation for water vapor inside heated concrete can be written as:

$$A\frac{dP_V}{dt} = \nabla B \nabla P_V + C \tag{1}$$

where P_V = pore pressure, t = time, A, B and C = parameters that depend on pore pressure, temperature, rate of increase in temperature, permeability of concrete, initial moisture content, and the isotherm used in the analysis. Isotherms are used to predict the liquid water inside concrete as a function of pore pressure for a constant temperature.

Finite element analysis is used to solve Equation 1 and compute the pore pressure distribution within the midsection of each segment along the length of the structural member. The resulting pore pressure is compared with the temperature dependent tensile strength of concrete as shown in Figure 1. Spalling is said to occur when the effective pore pressure (defined as the produce of porosity and pore pressure) exceeds the tensile strength of concrete; i.e., when the following expression is satisfied:

$$nP_V > f_{tT} \tag{2}$$

where n = porosity of concrete = $V_V + V_L$, f_{tT} = tensile strength of concrete for temperature, T, and V_V and V_L = volume fractions of water vapor and liquid water, respectively. Once spalling of concrete occurs, the reduced concrete section and the new boundary surface are considered in the thermal and strength analyses in subsequent time steps. In this way, the spalling and thermal calculations are coupled in the analysis.

In all spalling models, published thus far, the initial permeability (permeability at room temperature) is assumed to be uniformly distributed over the entire cross section of the beam. However, in practical situations, the concrete permeability varies within the cross section of the RC beam due to cracking patterns resulting

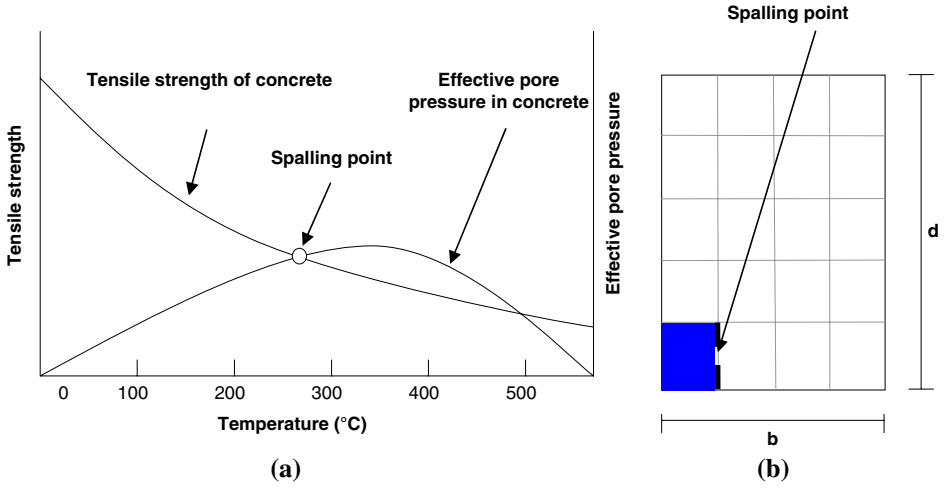

Figure 1. Illustration of spalling prediction in the proposed model. (a) Pore pressure and tensile strength variation. (b) Cross section.

from variation in bending moment and also due to curing conditions. The variation in the permeability of concrete can be assumed to change with the depth of the beam as given by the following equation:

$$k_0 = k_{top}\left\{\begin{array}{cc} 10^{2y/D} & yx \\ \underbrace{\left(10^{2y/D}\right)}_{\mathrm{I}}\underbrace{\left(10^{3\left(\frac{y-x}{D-x}\right)}\right)}_{\mathrm{II}} & y>x \end{array}\right\} \tag{3}$$

where k_0 = initial permeability of concrete, k_{top} = initial permeability in the top surface of the concrete section, D = total depth of concrete section, y = distance from the top most fibers of the concrete section, and x = depth of neutral axis under service loads.

The first and second terms in Equation 3 (terms I and II) account for the variation of permeability due to curing conditions and cracking in the concrete section, respectively. Equation 3 is developed based on the effect of cracking and damage on the permeability of concrete which can be generally given by [22, 24]:

$$k_{\text{damaged}} = k_{\text{undamaged}} \times 10^{\beta D} \tag{4}$$

where k_{damaged} and $k_{\text{undamaged}}$ = permeability of damaged and undamaged concrete, respectively, B = calibration parameter, and D = extent of damage.

Figure 2 shows the spatial variation of permeability for an RC beam with cross section of 300 mm × 500 mm. The permeability at the top of the beam (k_{top}) and the depth of the neutral axis were assumed to be 10^{-19} m^2, 100 mm, respectively. In the tension zone of the beam, the cracks in concrete becomes wider leading to higher values of permeability as shown in Figure 2. Further details on the model are given in Ref. [21].

The spalling submodel presented here is capable of predicting early and intermediate stages of spalling. Late spalling which occurs just prior to failure is not considered in the analysis since it results from degradation in strength and stiffness. However, such type of spalling, due to the fact that it occurs just prior failure, does not significantly influence the overall fire resistance of RC beams.

4. Experimental Studies

To validate the spalling submodel, spalling measurements were undertaken by conducting fire resistance experiments on one NSC and three HSC beams, designated as B2, B4, B5 and B6, respectively. The fire experiments were designed to investigate the effect of fire scenario, concrete strength (permeability), axial restraint and load on the extent of spalling. Further, the effect of spalling on the overall fire resistance was monitored by testing the beams up to failure.

4.1. Test Specimens

All four beams were of rectangular cross section of 406 × 254 mm and had 3960 mm length. The beams had 3 ϕ19 mm bars as tensile reinforcement and 2 ϕ

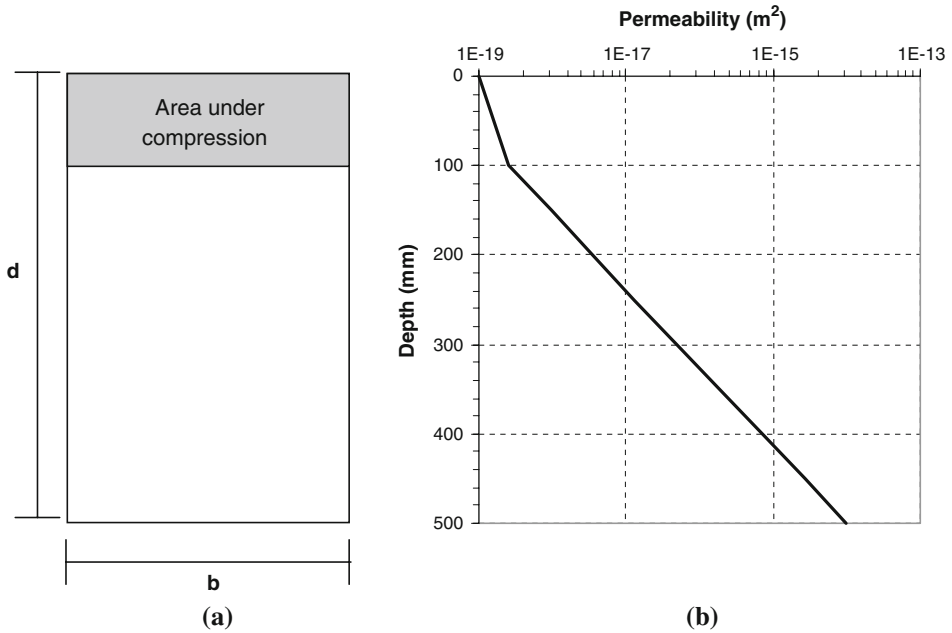

Figure 2. Variation of concrete permeability across the depth of a typical RC beam. (a) Cross section. (b) Permeability.

13 mm bars as compressive reinforcement. The shear reinforcement in the beams was ϕ6 mm stirrups with a spacing of 150 mm over the length of the beam. The steel of main reinforcing bars and stirrups had specified design yield strengths of 420 MPa and 280 MPa, respectively. Beams B2 and B6 were tested under axial restraint support conditions, while the remaining two beams (B4 and B5) were tested under simply supported end conditions. More details on the specifications of the beams are given in Table 1.

Table 1
Properties and Results for Tested RC Beams

Property	Beam B2	Beam B4	Beam B5	Beam B6
Strength	NSC	HSC	HSC	HSC
f'_c (MPa)	52.2	93.3	93.3	93.3
Loading ratio	0.55	0.55	0.65	0.55
Fire exposure	SF	SF	LF	LF
Support condition	Axially restrained	Simply supported	Simply supported	Axially restrained
Relative humidity (%)	81.1	86.6	91.8	92.5
Measured extent of spalling (end of test) (%)	1.5	3.2	7.0	8.7

Two batches of concrete were used for fabricating the beams. Beam B2 was fabricated from NSC mix (Batch 1), while beams B3 through B6 were fabricated from HSC mix (Batch 2). The two batches of concrete were made with general purpose, Type I Portland cement. The aggregates in both batches were of carbonate aggregate type (limestone). The mix proportions, per cubic meter of concrete, in the two batches consisted of:

	Batch 1	Batch 2
• Cement (kg/m3)	390	513
• Coarse aggregate (kg/m3)	1037	1078
• Fine aggregate (kg/m3)	830	684
• Water (kg/m3)	156	130
• Water reducing agent (kg/m3)	2	15
• Maximum aggregate size (mm)	10	10

Silica fume (43 kg/m3) was added to Batch 2 in order to obtain the targeted high strength concrete. The HSC beams were moist cured in the forms for 7 days, whereas the NSC beams were sealed in the forms for 7 days. Then all the specimens were lifted from the forms and stored in air maintained at about 25°C and 40% relative humidity.

The average compressive cylinder strength of the concrete, measured at 28 days and on the day of the testing, was 52.2 MPa and 58.2 MPa for NSC, and 93.3 MPa and 106 MPa for HSC, respectively. The concrete strength on the day of testing was found to be almost the same for the three HSC beams (B4 through B6). This can be explained by the fact that the increase in strength of HSC is generally not significant after 90 days of casting. The moisture condition (relative humidity) was measured on the day of the test using a relative humidity probe at a depth of 100 mm and at two different locations of the beam. The measured relative humidity values for the four tested beams are summarized in Table 1. It can be seen that the relative humidity of HSC beams is higher than that of the NSC beam. This can be attributed to slow drying in HSC beams resulting from the low permeability of HSC beams. The relative humidity in beams B5 and B6 was found to be higher than that in the remaining HSC beam (B4). This can be attributed to the fact that beams B5 and B6 were fabricated eight months after the fabrication of beam B4.

4.2. Instrumentation

The instrumentation of the beams included thermocouples, high temperature strain gauges, and displacement transducers. Type-K Chromel-alumel thermocouples, 0.91 mm thick, were installed at three different cross sections in each beam for measuring concrete and rebar temperatures. Also, five thermocouples were installed at the top side (unexposed side) of the beam. High temperature strain gauges were installed to measure strain in the reinforcing bars. Each of the beams, B1 through B4, was instrumented with 20 thermocouples and 4 high temperature strain gages. The remaining two beams (B5 and B6) were instrumented with 17 thermocouples and 2 high temperature strain gages. The deflection of each beam

is measured at mid-span as well as at the location of one of the two point loads, which were used for applying the external load on the beam during the fire test. More information on the location of the two point loads is given in the following section.

4.3. Test Procedure

The fire resistance tests were carried out by placing two RC beams in the furnace and exposing them to a desired fire exposure. The supported span of each beam was 3.66 m, with 2.44 m of the beam length exposed to fire. Beams B2 and B4 were tested by exposing them to a short design fire SF, while beams B5 and B6 were tested under long severe design fire LF. The time temperature curves for the two fire scenarios (SF and LF) are shown in Figure 3. It can be seen that both design fires have well defined decay phase with fire LF being more severe than fire SF.

All beams were tested under two point loads each of which is placed at about 1.4 m from the end supports. Beams B2, B4 and B6 were subjected to two point loads of 50 kN each, which is equal to 55% of the beam capacity (at room temperature) according to ACI 318 [31]. Beam B5 was subjected to two point loads of 60 kN or 65% of the beam capacity. Full details on the specimens, test procedure, test apparatus and instrumentation can be found elsewhere [32].

4.4. Test Results

Data collected from the above fire tests include rebar and concrete temperatures, strains, deflections, axial restraint force, fire induced spalling and failure time (fire resistance). However, only spalling measurements and observations are discussed in detail because the main focus of this paper is on fire induced spalling in RC beams.

The extent and nature of spalling was recorded by making visual observations through the windows of the furnace during the fire test and also by conducting

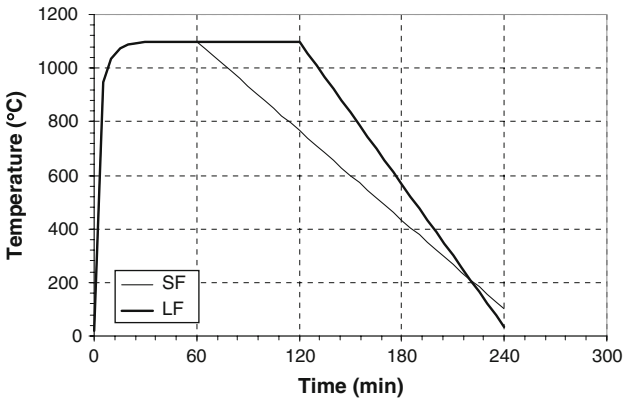

Figure 3. Time temperature curves for two design fires.

volumetric measurements of the beam after fire tests. The volumetric measurements were conducted by measuring the volume of the damaged beam and subtracting that from the original volume of the beam. The volumetric spalling ratio (defined as the ratio of spalled volume to the original volume of the beam) is given in Table 1.

In the case of NSC beam (B2), the extent of spalling was minimal or almost negligible throughout the fire exposure. Only prior to failure, there was some 'late spalling'. Post test, measurements indicated that the spalling volume in this NSC beam was only 1.5% of the original volume. In contrast, beams B4, B5 and B6 experienced spalling in early stages of fire exposure. The extent of spalling at the end of the test was 3.2%, 7.0% and 8.7% in HSC beams B4, B5 and B6, respectively. The higher extent of spalling observed in HSC beams can be attributed to the higher compactness or low permeability. This low permeability increases the pore pressure build up in HSC beams and when this pressure exceeds the tensile strength of concrete, chunks of concrete fall off from the surface of concrete.

In addition to permeability, load ratio and relative humidity were found to significantly influence the spalling in RC beams. Observations in the fire tests indicated that, for beams B2 and B4, spalling was not explosive and most of it is classified as intermediate and late spalling which occurred at intermediate and late stages of fire exposure. In contrast, there was significant and random explosive spalling in HSC beam B5 in the first 35 minutes after fire exposure. The severe extent of spalling observed in HSC beam B5 can be attributed to the higher load ratio this beam was subjected to and also to higher relative humidity in beam B5 as compared to beam B4.

Between the two HSC beams B5 and B6, more severe spalling occurred for the axially restrained beam B6, as compared to the simply supported beam B5, despite the fact that beam B6 was exposed to lower load ratio. This could be attributed to the fact that beam B6 was axially restrained and this led to the development of large axial restraint forces in that beam. The restraint forces alter the internal stresses in the beam (including higher tensile stresses in the lateral direction of the beam), and this enhances the conditions for fire induced spalling.

Figure 4 shows pictures of NSC beam B2 (exposed to design fire SF) and HSC beam B5 (exposed to design fire LF) after fire resistance tests. Also shown is a sketch of the beam section to illustrate the spalling that occurred at early stages of fire exposure in HSC beam B5. It can be seen that significant spalling occurred in the HSC beam as compared to the NSC beam. This can be attributed to the low permeability of HSC which significantly increases the fire induced spalling as discussed above. Although the HSC beam (B5) was exposed to fire from three sides, much of the early spalling was mainly observed on the upper area of both sides of the beam. The lack of spalling in bottom face of the beam (in spite of being exposed to fire) can be attributed to the cracking and curing conditions that significantly increase the permeability in the bottom part of the beam cross section as shown in Figure 2. The increased permeability (at the bottom face) facilitated the easy passage of steam pressure and this helped to limit the pore pressure build-up to levels below the critical limit at which spalling occurs.

Figure 4. Fire induced spalling in NSC beam B2 and HSC beam B5 under design fire exposure. (a) Spalling in RC beams after fire tests. (b) Spalling illustration at a cross section.

5. Model Validation

The validity of the spalling submodel is established by comparing spalling predictions with the measured values from fire tests for two HSC beams, B5 and B6, which experienced significant spalling. In these two beams significant spalling occurred at early stages of fire exposure (referred to as ''early spalling''). In both beams, the nature of spalling including the time at which spalling started and the approximate time at which spalling stopped were recorded. The extent of spalling at the end of the test was computed by measuring the volume of fire damaged beam. The extent of spalling is assumed to vary linearly between the time it started and the time it ended. These two beams experienced some ''late spalling'' just prior failure. However, most of the ''late spalling'' occurred in the midspan section of the beams and is not accounted for in the volumetric measurements and in the analysis (as ''late spalling'' has negligible effect on the overall behavior of the RC beam as discussed earlier).

The water permeability was measured in both beams prior to fire tests as per ASTM C1202 [33] using ''Chloride Penetration'' Test and was found to be about 10^{-21} m^2. The specimens used for permeability tests were cured under the same conditions as the top part of the beam and thus they are assumed to have the same permeability as that part of the beam. Gas permeability is generally higher than water permeability and can be higher in magnitude up to the order of 10^2 [34]. Thus, for the analysis, the permeability of water vapor in the top side of the concrete beams (k_{top}), which is required for pore pressure calculations, is assumed to be 10^{-19} m^2. The spatial variation of permeability in the beam cross section is assumed as given by Equation 3. For the two beams, the depth of the neutral axis under service loads (x in Equation 3) was found to be 90 mm. Based on the average spalling thickness measured in the tests, it is assumed in the analysis that the spalling depth (the thickness of spalled concrete) does not exceed 20 mm and 25 mm for beams B5 and B6, respectively. With these values as input parameters to the spalling submodel, the extent of spalling is evaluated as a function of fire exposure time for both beams.

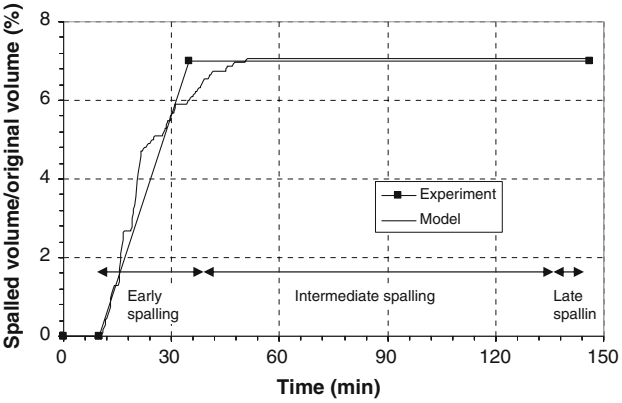

Figure 5. Measred and predicted extent of spalling as a function of time for beam B5.

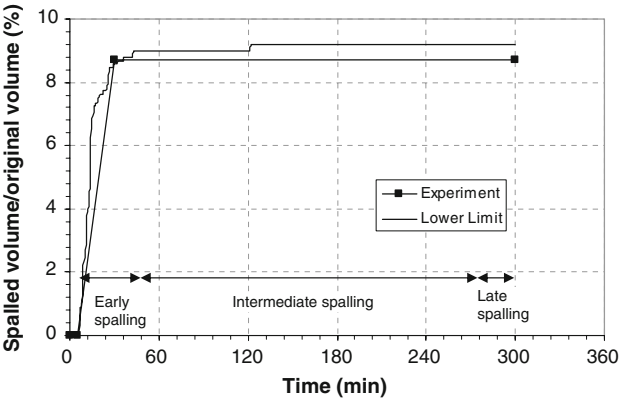

Figure 6. Measred and predicted extent of spalling as a function of time for beam B6.

The predicted values and times of spalling are compared with the measured values for beams B5 and B6 (which were exposed to design fire LF) in Figures 5 and 6, respectively. It can be seen that there is good agreement between the predicted and measured values in the entire range of fire exposure. For beam B5, the model predicts spalling to start at about 11 min and to stop at 50 min after fire exposure. The visual observations in the test indicated that spalling started and stopped at 10 and 35 min after fire exposure, respectively. Similarly, for beam B6, the measured start and end times of spalling were 5 min and 30 min, and the predicted times were 6.5 min and 122 min. These results indicate that the program predicts well the start time of spalling. In contrast, there is a variation between the predicted and the measured end time of spalling. This variation might be acceptable since the model predictions indicate that small amount of spalling occurs after 35 mins and 30 min

of fire exposure for beams B5 and B6, respectively. This can be attributed to the drying of concrete which reduces the developed pore pressure and hence decreases the spalling at later stages of fire. The model predicts slightly higher extent of spalling for beam B6, which is a conservative estimate. Overall, the spalling predictions match reasonably well with the measured values in early and intermediate stages of fire exposure for RC beams.

6. Case Studies

The validated numerical model was applied to investigate the influence of the main factors on the extent of spalling and also the effect of such spalling on the overall fire resistance of RC beams. The case studies presented in the paper provide a quantitative insight on the influence of concrete permeability and fire scenario on fire induced spalling in concrete beams and also the effect of spalling on the fire response of simply supported and axially restrained beams.

6.1. Analysis Details

For the analysis, two sets of RC beams (each set comprising of four RC beams) were selected and the parameters were varied over the full range. One beam in each set is made of NSC while the remaining three are made of HSC. The beams in the first set are simply supported (SS), while the beams in the second set are axially restrained (AR). The axial restraint stiffness (k) is assumed to be 50 kN/mm for the axially restrained beams. This value of the axial restraint stiffness is selected in such a way that it represents restraint conditions commonly encountered in practice [30]. Each beam is analyzed under four fire scenarios including two standard (ASTM E119 and ASTM E1529) and two design fire exposures. The analysis was carried out in 5 min time increments till failure occurred in the beam. The time to failure is taken as the fire resistance of the beam. The failure is said to occur when the strength limit state is exceeded in the beam. While the model is capable of applying either thermal, strength or deflection failure limit state, for the sake of simplicity, only strength limit state is considered here. Full details on the effect of different failure criteria on the fire resistance of RC beams are presented elsewhere [35]. Results from the analysis are summarized in Table 2.

All the analyzed RC beams are of rectangular cross section (300 mm × 500 mm) and have a span length of 6 m as shown in Figure 7. The compressive strength and permeability at top side (k_{top}) are assumed to be 30 MPa and 10^{-16} m^2 for NSC, and 100 MPa and 10^{-19} m^2 for HSC, respectively. The beams were reinforced with steel rebars having yield strength of 400 MPa. The depth of the neutral axis under service loads (x in Equation 3) was found to be 120 mm and 100 mm for NSC and HSC beams, respectively. The room temperature capacity of the analyzed beams was calculated based on ACI 318 provisions [31]. The applied loading on the beam, is calculated for a dead load to live load ratio of 2, based on ASCE 07 [36] provisions (1.2 dead load + 1.6 live load for room temperature calculation, and 1.2 dead load + 0.5 live load under fire conditions). For load calculations, the ultimate load at room temperature is equated to the room

Table 2
Summary of the Fire Resistance Values for the Analyzed Beams

Case	Beam designation	Concrete type	k_{top} (m^2)	Type of fire exposure	Fire resistance (minutes)	Extent of spalling (end of fire exposure) (%)
SS beam	BNS1	NSC	10^{-16}	ASTM E119	145	NS**
	BNS2			Hydrocarbon	120	NS
	BNS3			Design Fire I	NF*	NS
	BNS4			Design Fire II	NF	NS
	BHS1	HSC	10^{-19}	ASTM E119	115	12.27
	BHS2			Hydrocarbon	95	11.73
	BHS3			Design Fire I	95	10.67
	BHS4			Design Fire II	NF	6.0
AR beam	BNA1	NSC	10^{-16}	ASTM E119	175	NS
	BNA2			Hydrocarbon	150	NS
	BNA3			Design Fire I	NF	NS
	BNA4			Design Fire II	NF	NS
	BHA1	HSC	10^{-19}	ASTM E119	150	12.27
	BHA2			Hydrocarbon	130	11.73
	BHA3			Design Fire I	NF	10.67
	BHA4			Design Fire II	NF	6.0

* No failure; ** No spalling.

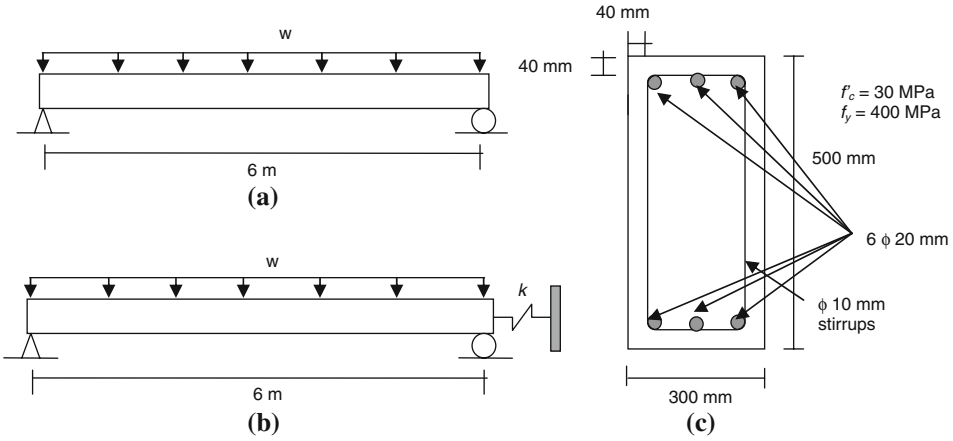

Figure 7. Cross section and elevation of RC beam used in the case studies. (a) Simply supported beam. (b) Axially restrained beam. (c) Cross section.

temperature capacity of each beam. The applied load was found to be 22.5 kN/m and 25.3 kN/m for NSC and HSC beams, respectively. For the analyzed beams, the spalling depth (thickness of concrete layer that spall off from the concrete section) is assumed not to exceed the clear concrete cover thickness (40 mm).

The temperature dependent properties that are important for establishing the fire response of RC structures include: thermal, mechanical and material specific properties such as permeability of concrete. For the fire resistance analysis of RC beams, the thermal and mechanical properties of NSC and reinforcing steel specified in the ASCE Manual [37] are used. However, since the material properties in the ASCE manual are only applicable for NSC, the material properties developed by Kodur et al. [38] are used for HSC.

In the cooling phase, the thermal properties of the constituent material (both concrete and steel) are assumed to be similar to those in the heating phase. For mechanical properties, linear interpolation between high temperature strength and residual strength is used to estimate the strength of both concrete and reinforcing steel in the cooling phase. The residual strengths for any concrete element or steel rebar are determined based on the maximum temperature attained in that element (or rebar). For concrete, the residual strength is assumed to be 75% of the high temperature strength determined at the maximum temperature attained in concrete. However, the residual strength of reinforcing steel is assumed based on the residual strength test conducted by Neves et al. [39] on reinforcing steel. Up to 500°C, residual strength of reinforcing steel is assumed to be similar to room temperature strength. However, the residual strength is assumed to decrease linearly with temperature till it reaches 70% of the room temperature strength at 800°C.

The main properties that influence spalling include permeability, tensile strength of concrete and isotherms which are used to predict the mass of liquid water inside concrete as a function of pore pressure and temperature. More details on spalling related properties are given in the Appendix.

To investigate the effect of fire scenario on concrete spalling and fire resistance, all the beams were analyzed under two standard fire scenarios, namely ASTM E119 [40] standard fire, and ASTM E1529 [41] hydrocarbon standard fire, and under two design fire scenarios; namely Fire I and Fire II, taken from Eurocode 1 [42]. There is no decay phase in the time temperature curves of standard fires. However, in realistic (design) fires, there always exist a decay phase, since the amount of fuel or ventilation runs out leading to burn out in the compartment.

The parametric fire time temperature curve proposed in Eurocode 1 [42], together with the recent modifications suggested by Feasey and Buchanan [43], are selected to represent the design fires, Fire I and Fire II. According to Eurocode 1, the design fire consists of a growth phase and a decay phase. Feasey and Buchanan [43] showed that both the growth and decay phases of the fire are influenced by compartment properties such as the fuel load, ventilation opening and wall linings. The time temperature curves for the two standard fire scenarios and the two design fire scenarios are shown in Figure 8.

6.2. Results and Discussion

Results from the computer runs are used evaluate the extent of spalling and its effect on the fire resistance in each beam and these are presented in Table 2 and Figures 9–11. The effect of each of the parameters on spalling and fire resistance is discussed below.

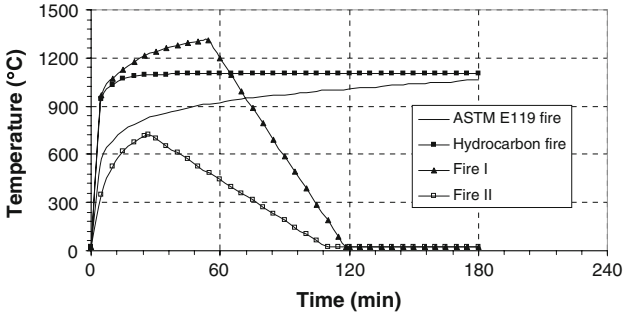

Figure 8. Fire scenarios used in the case studies.

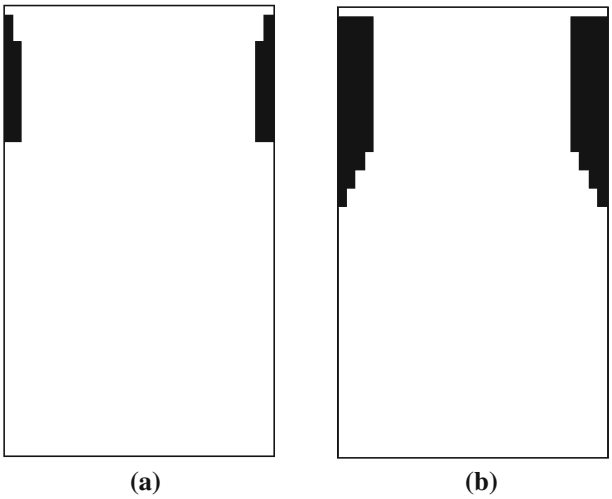

Figure 9. Spalling pattern in HSC beams exposed to ASTM E119 fire. (a) Concrete spalling after 20 min of fire exposure. (b) Concrete spalling after 40 min of fire exposure.

6.2.1. Effect of Permeability on Spalling. Results from the analysis (see Table 2) indicate that no spalling occurred in NSC beams (BNS1 to BNS4 and BNA1 to BNA4), whereas significant spalling occurred in HSC beams (BHS1 to BHS4 and BHA1 to BHA4). This can mainly be attributed to the low permeability in HSC beams, which prevents the passage of water vapor (steam), generated with increasing temperatures in concrete, leading to build-up of vapor pressure in concrete. When this vapor pressure exceeds the temperature dependent tensile strength of concrete, layers of concrete spall away from concrete (illustrated in Figure 1). However, in the case of NSC beams, the relatively higher level of permeability provides an easy mechanism for the water vapor to escape from the concrete. Thus, with increasing temperatures the pore pressure continuously dissipate in NSC beams and there is no significant vapor pressure build-up. Therefore, the

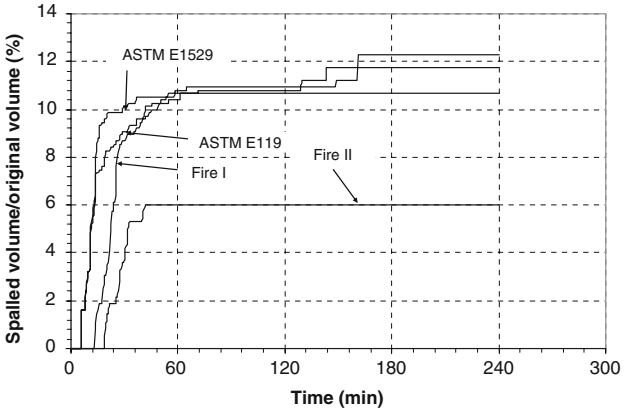

Figure 10. Effect of fire scenario on fire induced spalling in HSC beams.

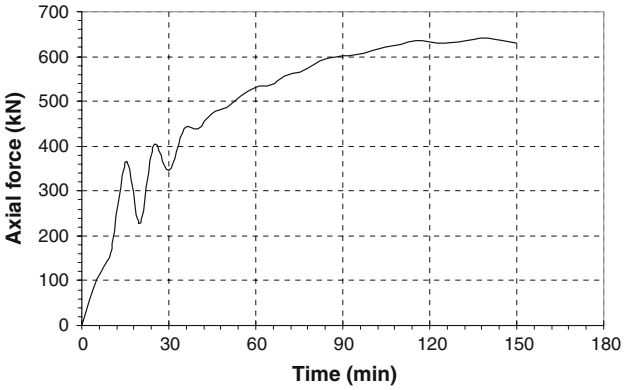

Figure 11. Axial restraint force developed in HSC beams exposed to ASTM E119 standard fire.

developed vapor pressure in NSC beams remains below the critical tensile strength value and thus no fire induced spalling occurs.

Figure 9 illustrates the spalled area in an HSC beam after 20 min and 40 min of fire exposure. It can be seen that the extent of spalling in the concrete section increases with fire exposure time. This can be attributed to the fact that once first layer of concrete spall away, the pore pressure will build-up subsequently in the inner layers of concrete leading to further spalling. Although HSC beams were exposed to fire from three sides, fire induced spalling occurred on the upper area of both sides of the beams. This can be mainly attributed to the higher permeability in the bottom part of the beam due to cracking in the tension zone (bottom part) and also due to worse curing conditions. The increased permeability relieves the fire induced pore pressure in the bottom part of the beam to levels below the critical limit at which spalling occurs.

6.2.2. Effect of Fire Scenario on Spalling. The effect of fire scenario on spalling in RC beams is illustrated in Figure 10 where the loss of concrete section is plotted as a function of time for different fire scenarios. It can be seen from the figure that the type of fire exposure has significant influence on the resulting spalling. The extent of spalling, in HSC beams exposed to ASTM E1529 hydrocarbon fire and severe design fire (Fire I), is higher than that in the HSC beams exposed to ASTM E119 fire and moderate fire (Fire II) at early stages of fire exposure time. This can be attributed to the high thermal gradient resulting from rapid increase in the temperature for the ASTM E1529 fire and Fire I at early stages of fire exposure as can be seen from fire time-temperature curves plotted in Figure 8.

At later stages of fire exposure, the rapid heating in the case of ASTM E1529 standard fire exposure results in early drying of the RC beam and hence the developed pore pressure is below the critical levels to cause spalling. This explains the lower extent of spalling (at later stages of fire exposure time) in the beams exposed to ASTM E1529 hydrocarbon fire as compared to those exposed to ASTM E119 standard fire (as can be seen in Table 2). Figure 10 also shows that the fire induced spalling in concrete is significantly influenced by the presence of the decay (cooling) phase in the time temperature curves of design fires. In the decay phase, the beam enters the cooling phase where the pore pressure decreases with fire exposure time due to the reduction in temperatures and thus no further spalling is predicted in concrete as can be seen from Figure 10.

6.2.3. Effect of Axial Restraint on Spalling. Based on fire test observations, previous researchers have reported that axial restraint has some influence on fire induced spalling in RC members. However, there have been no numerical studies to illustrate the effect of restraint on spalling. Studying the effect of axial restraint on concrete spalling is very complex and requires coupled structural and hydrothermal analysis. This coupling can be achieved through 3D microscopic finite element modeling of the RC structural member. Such microscopic modeling requires the knowledge of many high temperatures material properties that are not well know as discussed in Sec. 2. Therefore, the coupled effect of axial restraint and spalling of concrete is not accounted for in the current analysis. Despite the fact that the model does not account for the effect of axial restraint on spalling, axially restrained beams are included in the case study to illustrate the effect of spalling on the fire response of axially restrained RC beams.

A restrained RC beam, when exposed to fire, can develop significant axial force and this force varies with fire exposure time as can be seen from Figure 11. The fluctuation of the axial restraint force during the first 40 min of fire exposure can be attributed to fire induced spalling. Spalling reduces the axial stiffness and hence the axial restraint force in the beam. The axial restraint force starts to increase again due to the increase in rebar and concrete temperatures resulting from the exposure to fire. The development of this additional restraining force alters the internal stresses in the beam which may increase the tensile stresses in the plane of the beam cross section. The increased tensile stresses enhance the conditions for fire induced spalling [21].

6.2.4. Effect of Spalling on Fire Resistance. The fire induced spalling has significant effect on the fire resistance of RC beams as can be seen from Table 2. As an illustration, the fire resistance of beam BNS1 (made of NSC) is 145 min, whereas the fire resistance of beam BHS1 (made of HSC) is only 115 min. The reduction in the fire resistance for HSC beams results from two factors: the faster degradation of strength in high strength concrete and the occurrence of spalling in HSC beams. Spalling reduces the cross sectional area of the concrete and thus the moment capacity and stiffness of the beam. This results in early failure and lower fire resistance in HSC beams.

However, the spalling predictions, and related fire resistance, are dependent on the spatial variation of permeability within the beam cross section. Therefore, careful consideration should be given in evaluating spalling using numerical techniques. An illustration of the importance of spatial variation of permeability on fire resistance of RC beams is demonstrated below.

In the case of non-uniform permeability distribution across the beam cross section (as given by Equation 3), spalling occurs only in the upper part of the beam as discussed above. However, when uniform permeability distribution (across the beam cross section) was assumed, spalling occurred on both sides and on the bottom surface of the beam cross section and thus the fire resistance of a similar HSC beam was found to be 55 min [44]. Such value of fire resistance is much lower than the value computed in this study (115 min) and this can be attributed to the reduction in the concrete cover thickness resulting from spalling in the case of uniform permeability distribution [44]. The reduction in concrete cover thickness facilitates the heat penetration to the steel reinforcement and hence causes early failure in the RC beam.

7. Conclusions

Based on the results of this study, the following conclusions can be drawn:

- The permeability of concrete has significant influence on the fire induced spalling in RC beams. HSC beams, due to their low permeability, experiences higher spalling levels than NSC beams, where permeability is high.
- Spatial variation of permeability within a cross section of an RC beam has significant effect on the fire induced spalling and the fire resistance of the beam. Realistic spatial variation of permeability should be used for proper spalling prediction and also realistic fire resistance assessment of RC members.
- Type of fire exposure has significant influence on fire induced spalling. The extent of spalling can be higher under rapidly rising temperatures as encountered in hydrocarbon fires. In the case of design fire scenarios, spalling does not generally occur in the cooling phase of the fire.
- The extent of spalling has detrimental effect on fire resistance of RC beams. Thus, the fire resistance of HSC beams can be lower than that of NSC beams if spalling occurs in HSC.

Acknowledgment

The research, presented in this paper, is primarily supported by the Michigan State University Foundation, through Strategic Partnership Grant (Award No. SPG 71-4434), and the National Science Foundation CMMI program, Grant Number CMMI 0601178.

Appendix

For spalling calculations, the following material properties are assumed:

- *Isotherms*: The isotherms for the high strength concrete used in the analysis are shown in Figure 12 [20].
- *Permeability*: The variation of the permeability of concrete is assumed to follow the following expression [21]:

$$k_T = \left[10^{0.025(T-T_0)}\left(\frac{P_V}{P_0}\right)^{0.368}\right]k \tag{5}$$

  where k_T = intrinsic permeability of concrete at temperature T, k = initial intrinsic permeability of concrete at room temperature, P_0 = 101 325 Pa, P_V = pore pressure (Pa), and T_0 = initial temperature (°C).
- *Tensile strength*: The temperature dependent tensile strength of concrete is assumed as per Eurocode 2 [28] but with some modifications to avoid the conditions where the tensile strength becomes zero at relatively low temperatures (600°C). The model follows Eurocode 2 constitutive relationships for tensile strength of concrete up to 550°C. However, the Eurocode relationship is slightly modified for temperature range beyond 600°C. In this range, the tensile strength of concrete is assumed to decrease gradually until it reduces to zero at 1200°C. This modification is mostly to facilitate the numerical analysis (avoid convergence

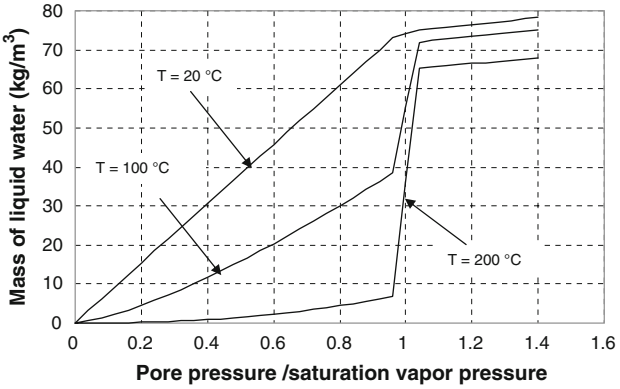

Figure 12. Isotherms for HSC used in the analysis.

problems). It should be noted that tensile strength of concrete at 550°C is only 10% of the room temperature tensile strength.

References

1. Kodur VKR (2000) Spalling in high strength concrete exposed to fire—concerns, causes, critical parameters and cures. ASCE structures congress proceedings, Philadelphia, USA, pp 1–8
2. Kodur VKR, Phan L (2007) Critical factors governing the fire performance of high strength concrete systems. Fire Saf J 42:482–488. doi:10.1016/j.firesaf.2006.10.006
3. Phan LT (1996) Fire performance of high-strength concrete. A report of the state-of-the-art. National Institute of Standards and Technology, Gaithersburg, MD, p 105
4. Diederichs U, Jumppanen UM, Schneider U (1995) High temperature properties and spalling behaviour of HSC. Proceedings of 4th Weimar workshop on HPC, HAB Weimar, Germany, pp 219–235
5. Kodur VR, Sultan MA (1998) Structural behaviour of high strength concrete columns exposed to fire. Proceedings: international symposium on high performance and reactive powder concrete, Sherbrooke, Quebec, vol 4, pp 217–232
6. Danielsen Ulf (1997) Marine concrete structures exposed to hydrocarbon fires. Report, SINTEF—The Norwegian Fire Research Institute, pp 56–76
7. Bilodeau A, Kodur VR, Hoff GC (2004) Optimization of the type and amount of polypropylene fibres for preventing the spalling of lightweight concrete subjected to hydrocarbon fire. Cement Concr Compos J 26(2):163–175. doi:10.1016/S0958-9465(03)00085-4
8. Hertz KD (2003) Limits of spalling of fire-exposed concrete. Fire Saf J 38:103–116. doi:10.1016/S0379-7112(02)00051-6
9. Fire Prevention (1997) Channel tunnel fire protection measures questioned after fire on HGV Wagon. Fire Prev 296
10. Kodur VR (2005) Guidelines for fire resistance design of high strength concrete columns. J Fire Prot Eng 15(2):93–106. doi:10.1177/1042391505047740
11. Mindess S, Young JF, Darwin D (2003) Concrete, 2nd edn. Prentice Hall, Pearson Education Inc, Upper Saddle River, NJ 07458
12. Phan LT (2007) Spalling and mechanical properties of high strength concrete at high temperature. Concrete under sever conditions: environment & loading, CONSEC'07, France
13. Han C, Hwang Y, Yang S, Gowripalan N (2005) Performance of spalling resistance of high performance concrete with polypropylene fiber contents and lateral confinement. Cement Concr Res 35(9):1747–1753
14. Hertz K (2003) Limits of spalling of fire-exposed concrete. Fire Saf J 38(2):103–116. doi:10.1016/S0379-7112(02)00051-6
15. Phan LT, Lawson JR, Davis FL (2000) Heating, spalling characteristics and residual properties of high performance concrete. Fifteenth meeting of the UJNR panel on fire research and safety, vol 2, NIST, USA
16. Park CK, Lee SH, Kim GD, Lee HK (2007) Effect of tie spacing and section size on fire resistance of high-strength concrete column. Concrete under sever conditions: environment & loading, CONSEC'07, France
17. Kodur VKR (2003) Fire resistance design guidelines for high strength concrete columns. NRCC-46116 ASCE/SFPE specialty conference of designing structures for fire and JFPE, Baltimore, MD, pp 1–11

18. Kodur VR, McGrath RC (2003) Fire endurance of high strength concrete columns. J Fire Technol 39(1):73–87. doi:10.1023/A:1021731327822
19. Kodur VKR, Cheng F, Wang T, Sultan MA (2003) Effect of strength and fiber reinforcement on fire resistance of high-strength concrete columns. J Struct Eng 129(2): 253–259. doi:10.1061/(ASCE)0733-9445(2003)129:2(253)
20. Bilodeau A, Kodur VKR, Hoff GC (2004) Optimization of the type and amount of polypropylene fibers for preventing the spalling of lightweight concrete subjected to hydrocarbon fire. Cement Concr Compos 26(2):163–174
21. Dwaikat MB, Kodur VK (2008) Hydrothermal model for predicting fire induced spalling in concrete structural systems. Fire Saf J (in press)
22. Gawin D, Majorana CE, Schrefler BA (1999) Numerical analysis of hygro-thermic behaviour and damage of concrete at high temperature. Mag Cohesive Frict Mater 4: 37–74. doi:10.1002/(SICI)1099-1484(199901)4:1<37::AID-CFM58>3.0.CO;2-S
23. Witek A, Gawin D, Pesavento F, Schrefler BA (2006) Finite element analysis of various methods for protection of concrete structures against spalling during fire. Comput Mech 39:271–292. doi:10.1007/s00466-005-0024-7
24. Gawin D, Pesavento F, Schrefler BA (2005) Towards prediction of the thermal spalling risk through a multi-phase porous media model of concrete. Comput Methods Appl Mech Eng 195:5707–5729. doi:10.1016/j.cma.2005.10.021
25. Tenchev RT, Li LY, Purkiss JA (2001) Finite element analysis of coupled heat and moisture transfer in concrete subjected to fire. Numer Heat Transfer A Appl 39(7):685–710
26. Davie CT, Pearce CJ, Bićanić N (2006) Coupled heat and moisture transport in concrete at elevated temperatures-effects of capillary pressure and adsorbed water. Numer Heat Transfer A Appl 49(8):733–763
27. Kodur VKR, Wang T, Cheng F (2004) Redicting the fire resistance behavior of high strength concrete columns. Cement Concr Compos 26(2):141–153
28. Eurocode 2 (2004) prEN1992-1-2: design of concrete structures. Part 1–2: general rules—structural fire design. Comité Europeén de Normalisation (CEN), Brussels
29. ACI Committee 216.1 (2007) Standard method for determining fire resistance of concrete and masonry construction assemblies. American Concrete Institute, Detroit
30. Dwaikat MB, Kodur VKR (2008) A numerical approach for modeling the fire induced restraint effects in reinforced concrete beams. Fire Saf J 43(4):291–307. doi:10.1016/j.firesaf.2007.08.003
31. ACI 318R-2008 (2008) Building code requirements for reinforced concrete. ACI 318-08 and commentary, American Concrete Institute, Detroit, MI
32. Dwaikat MB, Kodur VKR (2008) Response of restrained concrete beams under design fire exposure. J Struct Eng (Submitted)
33. ASTM C1202 (1997) Standard test method for electrical indication of concrete's ability to resist chloride ion penetration. American Society for Testing and Materials, West Conshohocken, PA
34. Neville AM (1996) Properties of concrete. John Wiley & Sons, Inc, New York, USA
35. Kodur VR, Dwaikat MB (2007) Performance-based fire safety design of reinforced concrete beams. J Fire Prot Eng 17(4):293–320. doi:10.1177/1042391507077198
36. ASCE 7-05 (2005) Minimum design loads for buildings and other structures. American Society of Civil Engineers, Reston, VA
37. Lie TT((1992) Structural fire protection. ASCE manuals and reports of engineering practice, No 78. American Society of Civil Engineers, New York
38. Kodur VKR, Wang T, Cheng F (2004) Predicting the fire resistance behavior of high strength concrete columns. Cement Concr Compos 26(2):141–153

39. Neves IC, Rodrigues JC, Loureiro AP (1996) Mechanical properties of reinforcing and prestressing steels after heating. J Mater Civ Eng 8(4):189–194. doi:10.1061/(ASCE)0899-1561(1996)8:4(189)
40. ASTM Test Method E119-08a (2008) Standard methods of fire test of building construction and materials. American Society for Testing and Materials, West Conshohocken, PA
41. ASTM Test Method E1529 (1993) Standard test methods for determining effects of large hydrocarbon pool fires on structural members and assemblies. American Society for Testing and Materials, West Conshohocken, PA
42. Eurocode 1 (1994) ENV 1991-2-2: basis of design and design actions on structures. Part 2–2: actions on structures exposed to fire. European Committee for Standardization
43. Feasey R, Buchanan AH (2002) Post flash-over fires for structural design. Fire Saf J 37(1):83–105. doi:10.1016/S0379-7112(01)00026-1
44. Dwaikat MB, Kodur VK (2008) Effect of fire scenario, restraint conditions, and spalling on the behavior of RC beams. Proceedings of fifth international conference on structures in fire, Singapore, pp. 369–379